



Performance study of three-phase induction motor driving a load

Oti Stephen Ejiofor¹, Nwosu Cajethan Abuchi², Nnadi Damian B N³,
Ogbonnaya I Okoro⁴

¹Department of Electrical Engineering, University of Nigeria, Nsukka, Enugu State Nigeria. E-mail: stephen.oti@unn.edu.ng

²Department of Electrical Engineering, University of Nigeria, Nsukka, Enugu State Nigeria. E-mail: cajethan.nwosu@unn.edu.ng

³Department of Electrical Engineering, University of Nigeria, Nsukka, Enugu State Nigeria. E-mail: damian.nnadi@unn.edu.ng

⁴Dept. of Elect./Electronics Engineering, Michael Okpara University of Agriculture, Umudike, Abia State, Nigeria. E-mail: oiokoro@yahoo.co.uk

Article History

Received: 11 April 2019

Accepted: 22 May 2019

Published: 1 June 2019

Citation

Oti Stephen Ejiofor, Nwosu Cajethan Abuchi, Nnadi Damian B N, Ogbonnaya I Okoro. Performance study of three-phase induction motor driving a load. *Discovery*, 2019, 55(282), 279-290

Publication License



© The Author(s) 2019. Open Access. This article is licensed under a [Creative Commons Attribution License 4.0 \(CC BY 4.0\)](https://creativecommons.org/licenses/by/4.0/).

General Note



Article is recommended to print as color digital version in recycled paper.

ABSTRACT

Induction motors are the most indispensable and widely used electric motors in industry. During start-up, loading and unloading operations, the asynchronous motor draws large currents, produce voltage dips and oscillatory torques. It is therefore important to model and study the asynchronous machine in order to predict these phenomena. Lots of work has been done on induction motor, ranging from transient and steady state responses to stability and performance studies. However, the effects of temperature variation during motor operations, variations in external rotor resistance and variable frequency drives have not received the desired attention. Hence, this work presents a step by step Matlab/Simulink implementation of a three-phase induction motor driving a load. Herein, a model of 126hp rated three-phase induction motor driving step input loads at different levels was demonstrated. Motor parameters were varied in order to study the effects of such variations on transient response and general performance of the

motor. The electromechanical torque and motor speed responses of the motor were examined. Consequently, recommendations for optimal motor operation were proposed.

Keywords: Asynchronous, Matlab/Simulink, Transient, Performance, Load, Step input

1. INTRODUCTION

The three-phase induction motor is the most common of all industrial motors. The use of induction motors has increased tremendously since the day of its invention. They are being used as actuators in various industrial processes, robotics, house appliances and other similar applications. The growing popularity of the individual drive system in small workspaces, and the increasing use of portable electric tools, has stimulated development of motors, which, though of very small size, are of excellent electrical and mechanical design, and form miniature power units of great reliability and good performance [1].

During start-up, loading, unloading and other severe motoring operations, the asynchronous motor draws large currents, produce voltage dips, oscillatory torques and can even generate harmonics in the power system [2]. It is therefore important to be able to model the asynchronous machine in order to predict these phenomena.

In the past, researchers have developed their own software packages for dynamic modeling of induction motor [3]. It is unnecessary to develop user-written software for dynamic model of induction motor when proprietary software package such as Matlab/Simulink, licensed by MathWorks which makes simulation design easy and more efficient is easily available.

Though some researchers have done similar work to this topic [2, 4, 5, 6, 7, 8], most of them simulated the induction motor model under no load condition while others with a specific load. The induction motor static model as developed in [4] did not take into consideration the effect of the load inertia. The load inertia is a very significant factor when it comes to stability and motor performance studies [5]. While [6] did a work on induction generator operating at a speed of 6600rpm, [7] studied the induction machine driving a pump load considering the steady and transient states in the analysis. Computer simulation of induction machine coupled to a mechanical load was well analyzed in [8] but in [9], 7.5kW squirrel cage induction motor used for study was modelled using Simulink block and the work neglected number of poles in rotor speed equation, it varied only the stator resistance in the motor performance study. Presently, this work is aimed at modelling and simulation of 126-hp rated, three-phase induction motor driving different load levels of 0Nm, 100Nm, 550Nm and 1200Nm using Simulink blocks. Furthermore, the stator and rotor impedance of the motor were also varied so as to achieve optimal operation which guarantees an optimal use of the three phase induction motor in different industrial applications. It is known that the speed of rotation of the d-q axis can be arbitrary although there are three preferred speeds or reference frames as presented in [2]:

- (a) The stationary reference frame where the d-q axes do not rotate.
- (b) The rotor reference frame where the d-q axes rotate at rotor speed.
- (c) The synchronously rotating reference frame where the d-q axes rotate at synchronous speed.

Meanwhile, the following assumptions as noted in [9] were made to derive the dynamic model:

- i Uniform air gap.
- ii Balanced rotor and stator windings, with sinusoidally distributed mmf.
- iii Saturation, eddy current and temperature effects are neglected
- iv Skin-effect neglected

Direct quadrature transformation of three phase induction motor

In balanced three-phase circuits, application of the dq transform reduces the three AC quantities to two DC quantities [11]. The two stages used to achieve dq transformation are the Clarke's and the Park's transformation.

Clarke's Transformation

Three-phase voltages varying in time along the axes a, b, and c, can be algebraically transformed into two-phase voltages, varying in time along the axes α and β by the following transformation matrix [12].

$$\begin{bmatrix} F\alpha \\ F\beta \end{bmatrix} = \frac{2}{3} \begin{bmatrix} 1 & -1/2 & -1/2 \\ 0 & \sqrt{3}/2 & -\sqrt{3}/2 \end{bmatrix} \begin{bmatrix} Fa \\ Fb \\ Fc \end{bmatrix} \dots\dots\dots(1)$$

The inverse transformation can also be obtained to transform the quantities back from two-phase to three-phase:

$$\begin{bmatrix} Fa \\ Fb \\ Fc \end{bmatrix} = \frac{2}{3} \begin{bmatrix} 1 & 0 \\ -1/2 & \sqrt{3}/2 \\ -1/2 & -\sqrt{3}/2 \end{bmatrix} \begin{bmatrix} F\alpha \\ F\beta \end{bmatrix} \dots\dots\dots (2)$$

Park's Transformation

The two-axis orthogonal stationary reference frame quantities are transformed into rotating reference frame quantities using the park's transformation. This is expressed by the following transformation matrix:

$$\begin{bmatrix} Fd \\ Fq \end{bmatrix} = \begin{bmatrix} \cos\theta & \sin\theta \\ -\sin\theta & \cos\theta \end{bmatrix} \begin{bmatrix} F\alpha \\ F\beta \end{bmatrix} \dots\dots\dots (3)$$

The inverse transformation can also be obtained to transform the quantities back from two-phase rotating to two-phase stationary frame as follows [13]:

$$\begin{bmatrix} F\alpha \\ F\beta \end{bmatrix} = \begin{bmatrix} \cos\theta & -\sin\theta \\ \sin\theta & \cos\theta \end{bmatrix} \begin{bmatrix} Fd \\ Fq \end{bmatrix} \dots\dots\dots (4)$$

Dynamic Model equations for 3-phase induction motor

The dynamic model of induction motor in arbitrary reference frame can be represented by using flux linkages as variables. The model equations can be generated from the dq equivalent circuit of the induction machine [11, 14]. Figures 1 and 2 below show the equivalent circuit of the induction machine.

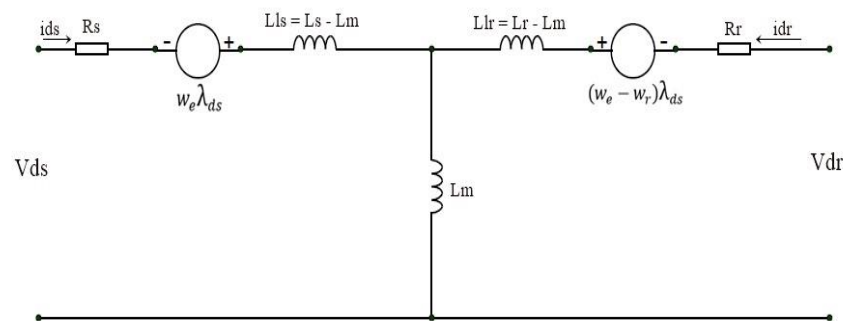


Figure 1 d-axis equivalent circuit of the Induction Motor

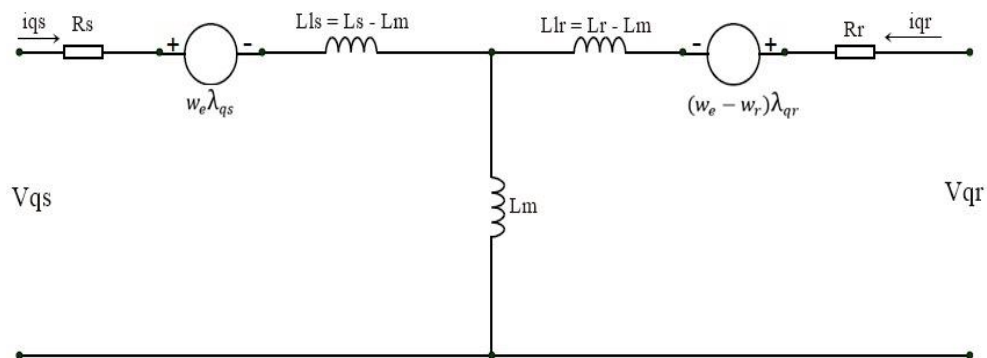


Figure 2 q-axis equivalent circuit of the Induction Motor

Flux Linkage Equations

The flux linkage equations associated with this circuit can be found as follows [2]:

$$\frac{d\lambda_{qs}}{dt} = \omega_b \left[V_{qs} - \frac{\omega_e}{\omega_b} \lambda_{ds} + \frac{R_s}{X_{ls}} (\lambda_{mq} - \lambda_{qs}) \right] \dots \dots \dots (5)$$

$$\frac{d\lambda_{ds}}{dt} = \omega_b \left[V_{ds} - \frac{\omega_e}{\omega_b} \lambda_{qs} + \frac{R_s}{X_{ls}} (\lambda_{md} - \lambda_{ds}) \right] \dots \dots \dots (6)$$

$$\frac{d\lambda_{qr}}{dt} = \omega_b \left[V_{qr} - \frac{(\omega_e - \omega_r)}{\omega_b} \lambda_{dr} + \frac{R_r}{X_{lr}} (\lambda_{mq} - \lambda_{qr}) \right] \dots \dots \dots (7)$$

$$\frac{d\lambda_{dr}}{dt} = \omega_b \left[V_{dr} - \frac{(\omega_e - \omega_r)}{\omega_b} \lambda_{qr} + \frac{R_r}{X_{lr}} (\lambda_{mq} - \lambda_{dr}) \right] \dots \dots \dots (8)$$

Where

$$\lambda_{mq} = X_{ml} \left[\frac{\lambda_{qs}}{X_{ls}} + \frac{\lambda_{qr}}{X_{lr}} \right] \dots \dots \dots (9)$$

$$\lambda_{md} = X_{ml} \left[\frac{\lambda_{ds}}{X_{ls}} + \frac{\lambda_{dr}}{X_{lr}} \right] \dots \dots \dots (10)$$

$$X_{ml} = \frac{1}{\left[\frac{1}{X_m} + \frac{1}{X_{ls}} + \frac{1}{X_{lr}} \right]} \dots \dots \dots (11)$$

Then substituting the values of the flux linkages to find the currents;

$$I_{qs} = \frac{1}{X_{ls}} [\lambda_{qs} - \lambda_{mq}] \dots \dots \dots (12)$$

$$I_{ds} = \frac{1}{X_{ls}} [\lambda_{ds} - \lambda_{md}] \dots \dots \dots (13)$$

$$I_{qr} = \frac{1}{X_{lr}} [\lambda_{qr} - \lambda_{mq}] \dots \dots \dots (14)$$

$$I_{dr} = \frac{1}{X_{lr}} [\lambda_{dr} - \lambda_{md}] \dots \dots \dots (15)$$

Torque and Rotor Speed Equation

Based on the above equations, the torque and rotor speed can be determined as follows [14]:

$$T_e = \frac{3}{2} \left(\frac{P}{2} \right) \frac{1}{\omega_b} [\lambda_{ds} I_{qs} - \lambda_{qs} I_{ds}] \dots \dots \dots (16)$$

$$\omega_r = \int \frac{P}{2J} (T_e - T_l) \dots \dots \dots (17)$$

For squirrel cage induction motor, the rotor voltages V_{qr} and V_{dr} in the flux equations are set to zero since the rotor cage bars are shorted [1]. The symbols as used above can be defined as follows;

P = number of poles

ω_b = motor angular electrical base frequency,

ω_r = rotor angular electrical speed,

R_s = stator resistance,

X_{ls} = stator reactance,

R_r = rotor referred resistance,

X_{lr} = rotor referred reactance,

X_m = magnetizing reactance,

X_{ml} = machine equivalent stator reactance,

T_e = electromechanical torque,

TL = externally applied mechanical load torque,

J = Moment of inertia,

V_{qs} = q-axis stator voltage,

V_{ds} = d-axis stator voltage,

V_{dr} = d-axis referred rotor voltage,

V_{qr} = q-axis referred rotor voltage,

I_{qs} = q-axis stator current,

I_{ds} = d-axis stator current,

I_{qr} = q-axis referred rotor current,

I_{dr} = d-axis referred rotor current

Simulink Implementation of the Induction Motor Sub-Models

The derived equations represented above are modeled using the subsystem approach in Simulink. However, the sub-models of the various subsystems in the complete Simulink model are shown below;

Voltage transformation Sub-model

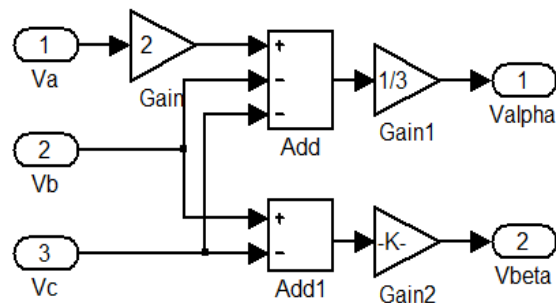


Figure 3 Clark's transformation

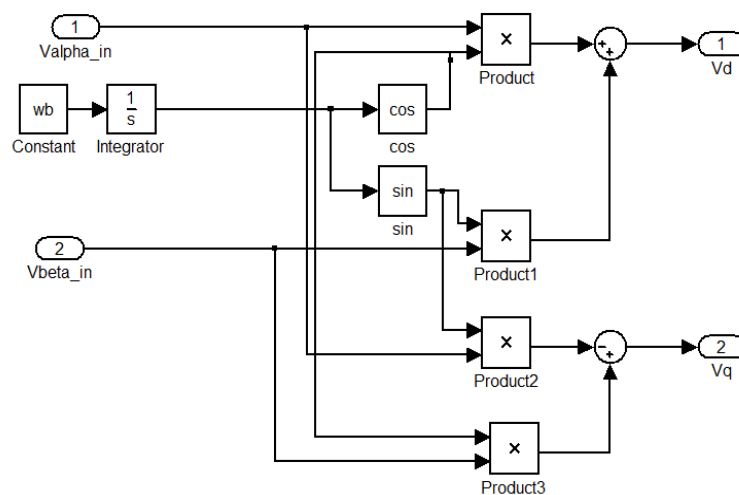
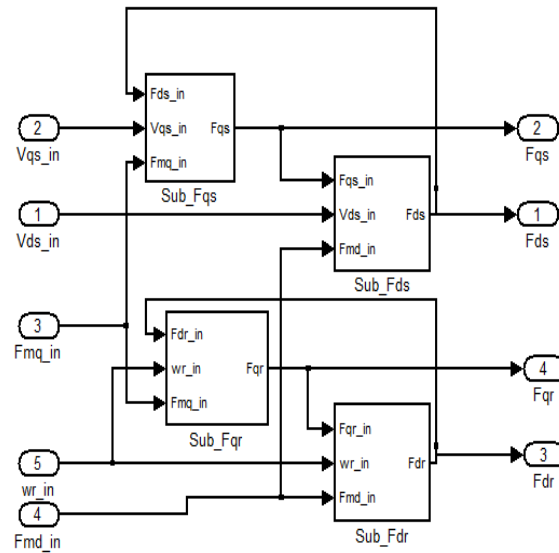
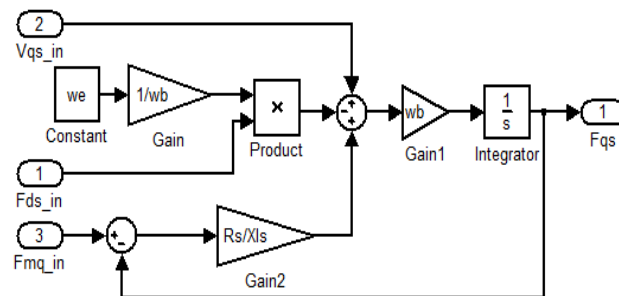
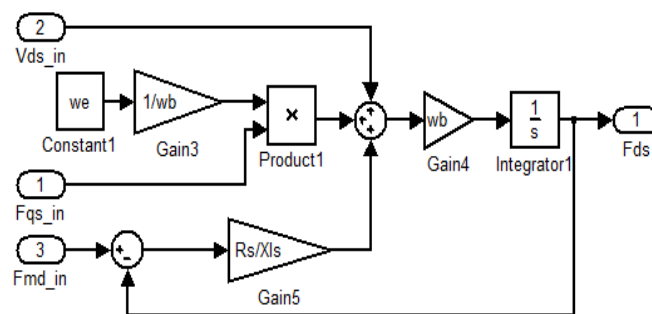


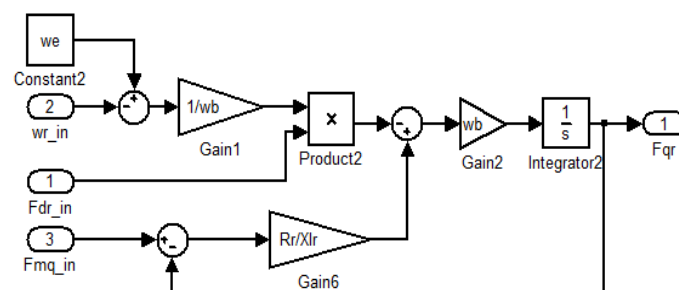
Figure 4 Parks transformation

Flux linkage Sub-model**Figure 5** Flux linkage sub-model

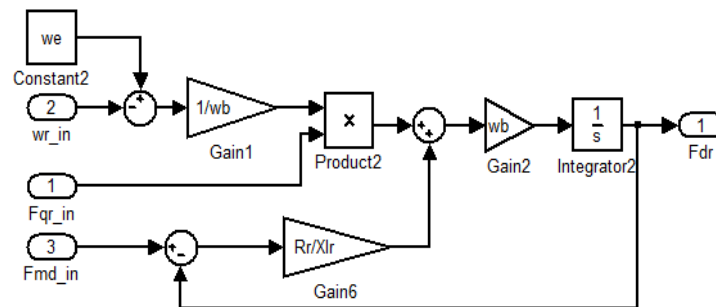
(i)



(ii)



(iii)



(iv)

Figure 6 (i)-(iv) represent implementation of the equations (5)-(8) respectively

Current sub-model

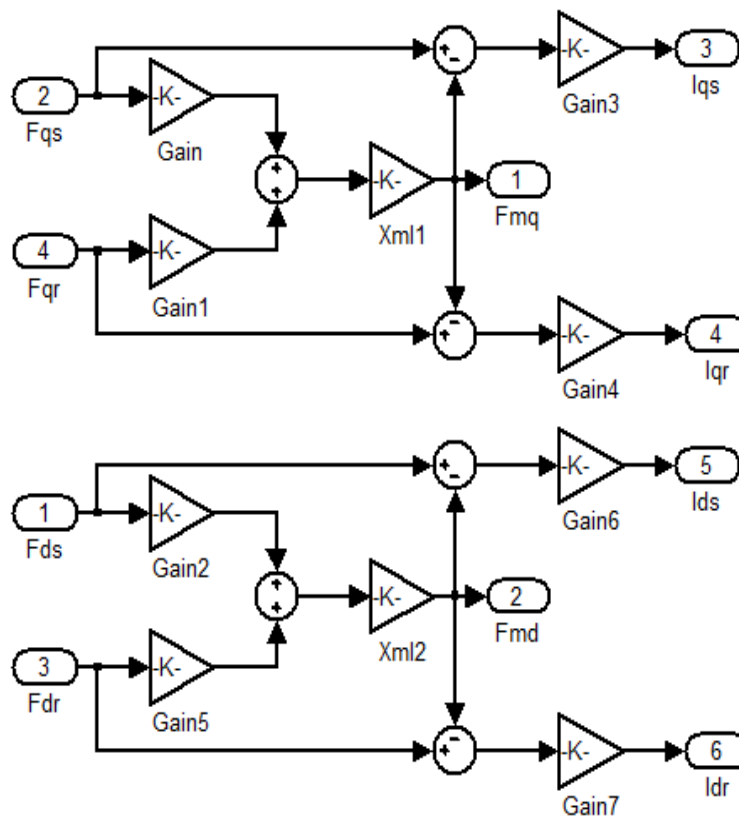


Figure 7 This block calculates the currents I_{qs} , I_{ds} , I_{qr} , I_{dr} , and the fluxes λ_{mq} , λ_{md} .

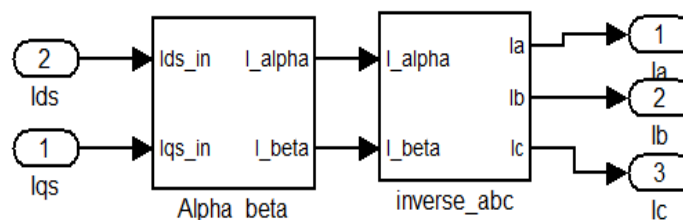


Figure 8 This block implements the inverse park and Clarke transformation.

Motor speed and Electro-mechanical torque Sub-model

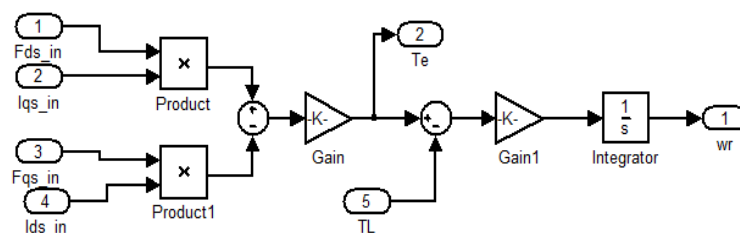


Figure 9 The implementation of the torque equation T_e (16) and the angular speed equation ω_r (17)

Complete Simulink block Implementation of the three phase induction motor

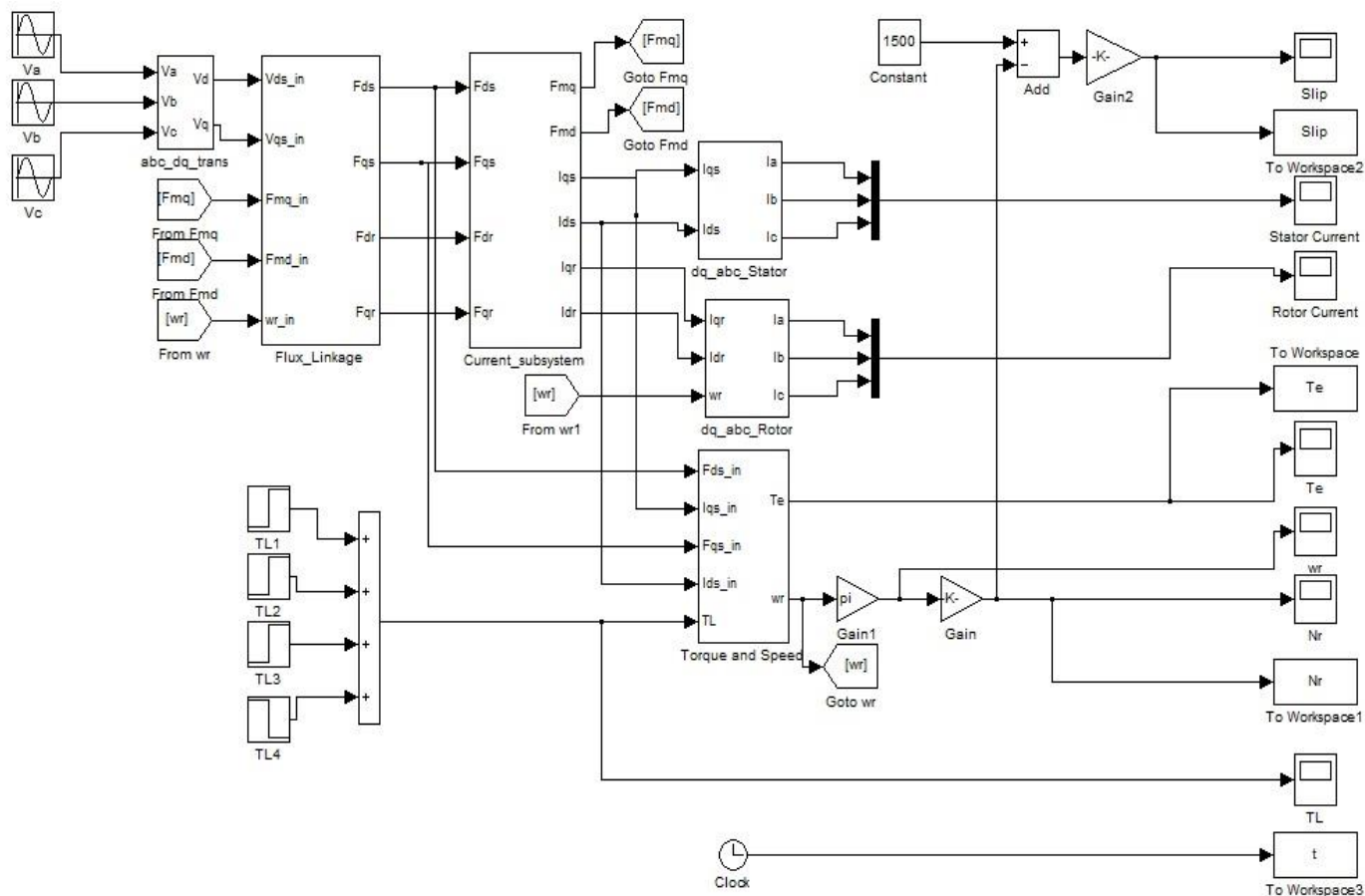


Figure 10 Complete Simulink block model of three phase induction motor

Simulation of the model

The induction motor rated parameters are listed in table 1.

Table 1 Induction motor rated parameters

Parameter	Symbol	Value
Phase Voltage	V_p	220V
Frequency	f	50Hz
No. of Poles	P	4
Moment of Inertia	J	0.089kg.m ²

Rotor resistance	R_r	0.816 Ω
Stator resistance	R_s	0.435 Ω
Rotor reactance	X_{lr}	0.754 Ω
Stator reactance	X_{ls}	0.754 Ω
Magnetizing reactance	X_m	26.13 Ω
Base angular frequency	ω_b	314.2rad/s

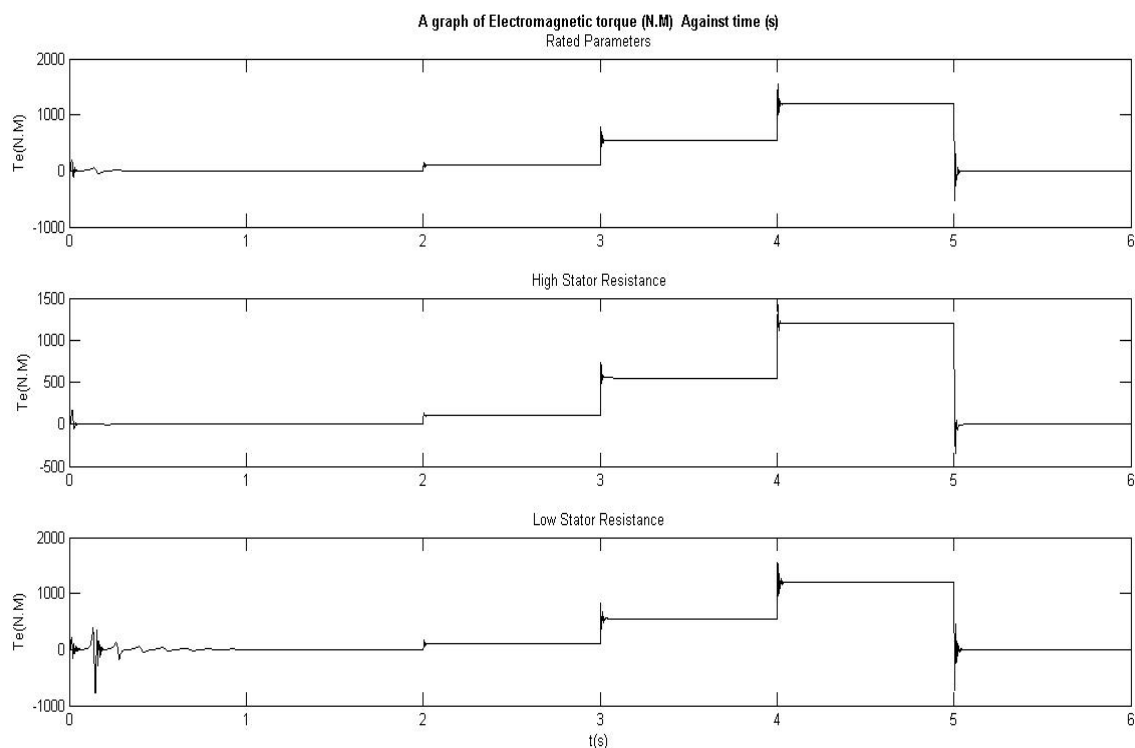
The induction motor was simulated with variable load stepped torque as shown in table 2. Also, the performance of this induction motor with different rotor and stator resistance and reactance values were simulated. Table 3 contains different rotor and stator parameters used in this work.

Table 2 Different motor loading conditions

Motor Loading	TL (N.M)
No Load	0
Low Load	100
Medium Load	550
Rated Load	1200

Table 3 Values for motor variable parameters

Variable Parameters		
Parameters	Resistance (Ω)	Reactance (Ω)
Low stator	0.16	0.016
High stator	1.0	2.1
Low rotor	0.1	0.016
High rotor	2.0	2.1



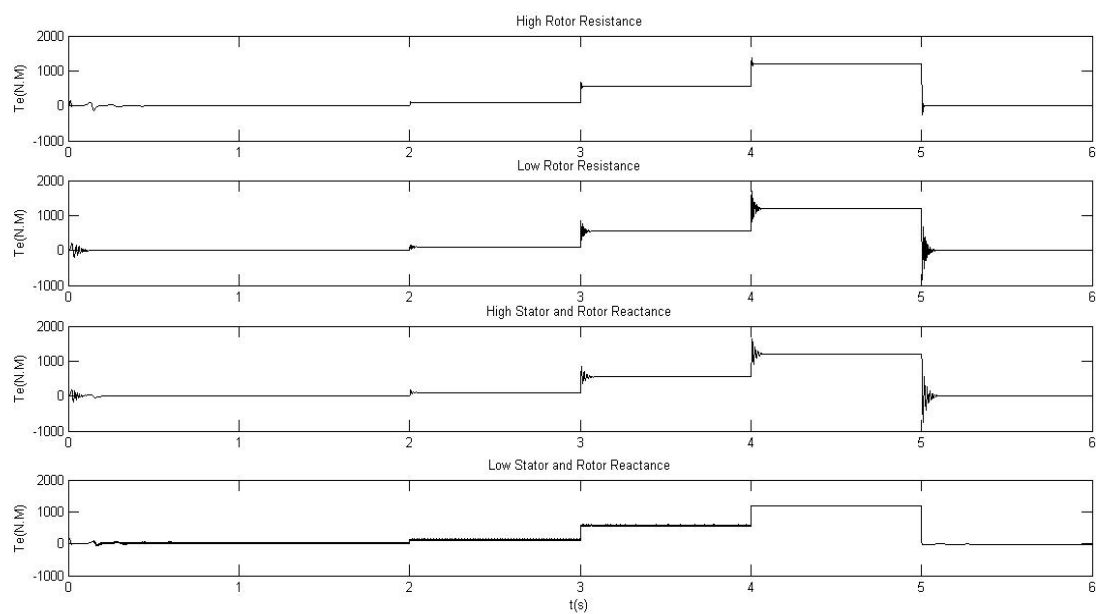
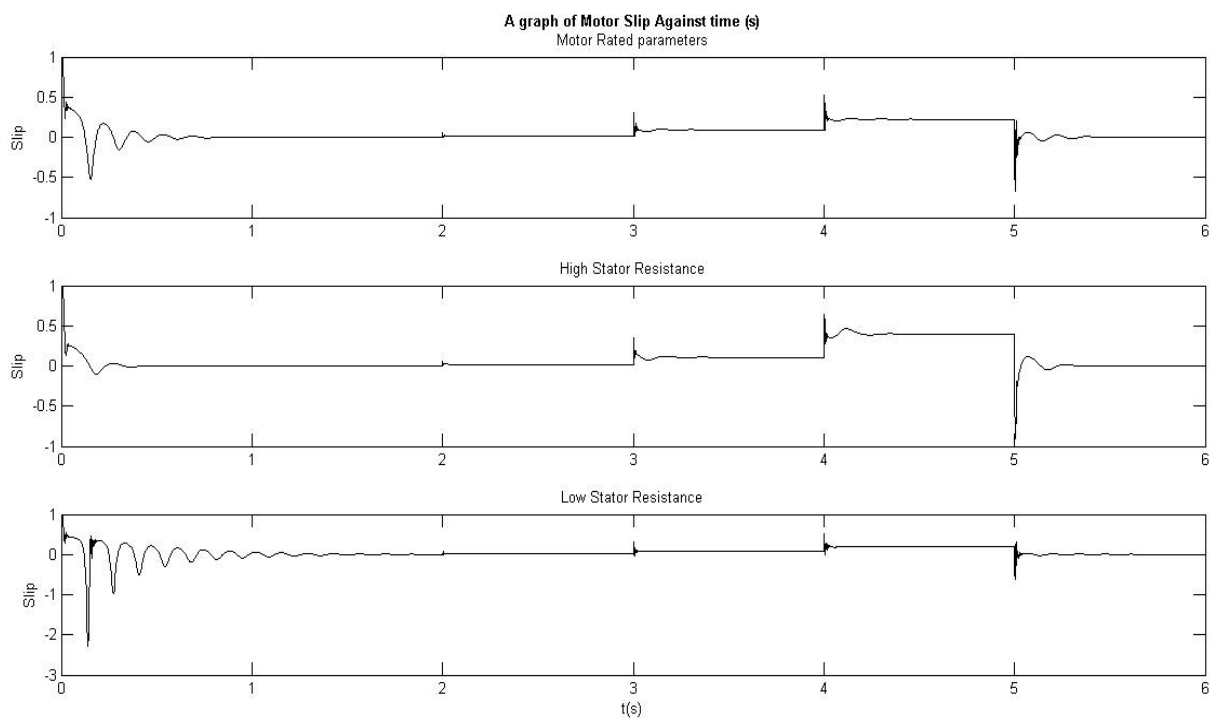


Figure 11 Graph of Electromagnetic torque (N.m) against time (s)



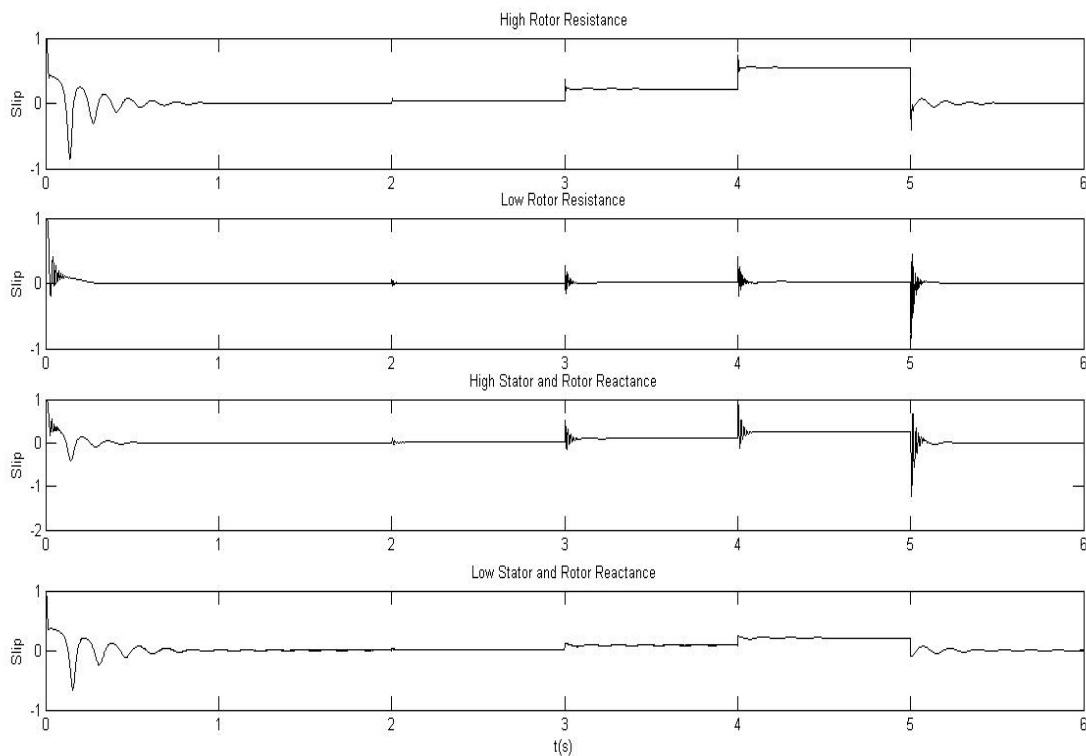


Figure 12 Graph of Motor Slip against time (s)

2. DISCUSSION OF SIMULATION RESULTS

From the above simulation results, overshoot in electromagnetic torque was observed across all parameter variations in the motor as shown in figure 11 although it occurred higher in the cases of low stator resistance, high stator and rotor reactance, and high rotor resistance parameter values. Precisely, a very high overshoot was observed in motor torque both in starting and load step inputs at low stator resistance. This resulted to the motor slip spanning between values of 1 and -2.3 as shown in figure 12. This overshoot is about four times its rated value. However, large increase in motor slip due to applied load input was observed with either high stator or rotor resistance values. Also, the motor experienced jerky start with high stator resistance value. The motor transient lasted for a longer time in low stator resistance than in high stator resistance value. A low overshoot was also observed in this high stator resistance value. Transient period at low reactance lasted longer compared to that of the rated and high reactance values. That notwithstanding, both stator and rotor reactance increase are capable of causing jerky motor start amidst high overshoot at load step inputs.

3. CONCLUSION

A 126-hp rated, three-phase induction motor with stepped load at different levels of 0Nm, 100Nm, 550Nm and 1200Nm was modelled in this work by the use of Simulink blocks in Matlab. The motor stator and rotor parameters were varied for motor performance studies. From the simulation results, during motor start-up, loading and unloading conditions, the asynchronous motor draws large currents, produce voltage dips, oscillatory torque. These results vary with different motor parameters. Low stator resistance, high motor reactance, and high rotor resistance parameter values cause high overshoot in motor torque and speed. However, low stator resistance causes increased motor transient time during motor start and step inputs. Also, High rotor resistance causes wide variations in speed during load step inputs. Increased motor reactance, whether rotor or stator, causes high overshoot, jerky start and decreased power factor. Following the observed characteristics it would be very pertinent to recommend that; (i) Soft starting of the induction motor should be adopted to avoid voltage dips and machine breakdown. This can be achieved through induction motor star-delta starting technique. (ii) Enough vents and cooling system should be provided in the motor to decrease the temperature of the motor during operation. Hence, preventing rise in stator resistance. (iii) Due to the wide variations in speed during load step inputs, external rotor resistance which is often used to achieve maximum torque at different slip should be disconnected during motor operation for efficient and good motor torque speed characteristics. (iv) In variable frequency drive (VFD), the operating frequency to rated frequency ratio should be maintained at a value less than unity during motor starting. This

operating state will cause a decrease in stator and rotor reactance. Hence, reduced jerky motor start with decreased overshoot and improved power factor is achieved.

REFERENCE

1. P. Arnold, L. Alger and E. Robert, "The History of Induction Motors in America," IEEE Trans, vol. 64, pp. 1380-1383, September, 1976.
2. P. C. Krause and C. H. Thomas, "Simulation of Symmetric induction machinery," IEEE Trans. Power Apparatus and Systems, Vol. PAS-84, no. 11, pp. 1038-1053, 1965.
3. A. W. Leedy, "Simulink / MATLAB Dynamic Induction Motor Model for Use as A Teaching and Research Tool," International Journal of Soft Computing and Engineering (IJSCE), vol. 3, no. 4, pp. 2231-2307, September, 2013.
4. Y. Mansour, "Voltage stability analysis using generic dynamic load models," IEEE Trans. on Power Systems, vol. 9, no. 14, pp. 479-493, February 1994.
5. T. Aboul-Seoud and J. Jatskevich, "Dynamic Modeling of Induction Motor loads for Transient Voltage Stability Studies," in IEEE Electrical Power & Energy Conference, Canada, 2008.
6. L. J. Phukon and N. Baruah, "A Generalized Matlab Simulink Model of a Three Phase Induction Motor," International Journal of Innovative Research in Science, Engineering and Technology, vol. 4, pp. 2926-2934, May 2015.
7. O.I. Okoro, "Steady state and transient analysis of induction motor driving a pump load", Nigerian Journal of Technology, Vol.22, no.1, pp46-53, March 2003.
8. O.I. Okoro, "Computer simulation of induction machine coupled to a mechanical load", Nigerian Journal of Engineering Management, NJEM, Vol.4, no.4, pp.28-38. 2003.
9. K. L. Shi, T. F. Chan, Y. K. Wong and S. L. Ho, "Modelling and Simulation of the Three-Phase Induction Motor using Simulink," International Journal of Electrical Engineering Education, vol. 36, pp. 163-172, 1999.
10. P. L. Ratnani and A. G. Thosar, "Mathematical Modelling of an 3 Phase Induction Motor Using MATLAB/Simulink," International Journal of Modern Engineering Research (IJMER), vol. 4, no. 6, p. 2249-6645, June 2014.
11. A. Oliveira, A. Monteiro, M. L. Aguiar and D. P. Gonzaga, "Extended DQ Transformation for Vectorial Control Applications of Non-sinusoidal Permanent Magnet AC Machines," in IEEE 36th Power Electronics Specialists Conference, Recife, 2005.
12. P. M. Menghal, A. J. Laxmi and N. Mukhesh, "Dynamic simulation of induction motor drive using neuro controller," International Journal on recent trends in Engineering and Technology, vol. 10, pp. 32-40, 2014.
13. S. Boora, S. K. Agarwal and K. S. Sandhu, "Dynamic d-q Modelling of Three-Phase Asynchronous Machine Using Matlab," International Journal of Advanced Research in Electrical, Electronics and Instrumentation Engineering, vol. 2, no. 8, pp. 3942-3951, August 2013.
14. M. Kumar, P. Babu and S. Ramprasad, "Four Quadrant Operation of Direct Torque Control-SVPWM Based Three Phase Induction Motor Drive in MATLAB/Simulink Environment," Proceedings of the IEEE International Conference on Advanced Communication Control and Computing Technologies (ICACCCT), p. 397 – 402, 2012.